

Electronic Supplementary Material

Thin platelet- like COF Nanocomposites for Blood Brain Barrier Transport and Inhibition of Brain Metastasis from Renal Cancer

Guiyang Zhang^{a,d,#}, Bo Jiang^{b,#}, Chunyong Wu^{c,#}, Yanfeng Liu^a, Yidan He^c, Xin Huang^a, Wei Chen^b, Kai Xi^{*a}, Hongqian Guo^{*b}, Xiaozhi Zhao^{*b}, and Xudong Jia^{*a}

^a School of Chemistry and Chemical Engineering, Nanjing University, Jiangsu 210023, China

^b Department of Urology, Drum Tower Hospital, Medical School of Nanjing University, Institute of Urology, Nanjing University, 321 Zhongshan Road, Nanjing, 210008, Jiangsu, PR China

^c Department of Pharmaceutical Analysis, China Pharmaceutical University, Nanjing 210009, China

^d Department of Pharmacology, School of Basic Medical Sciences, Anhui Medical University, Hefei 230032, China

[#] These authors contributed equally to this work.

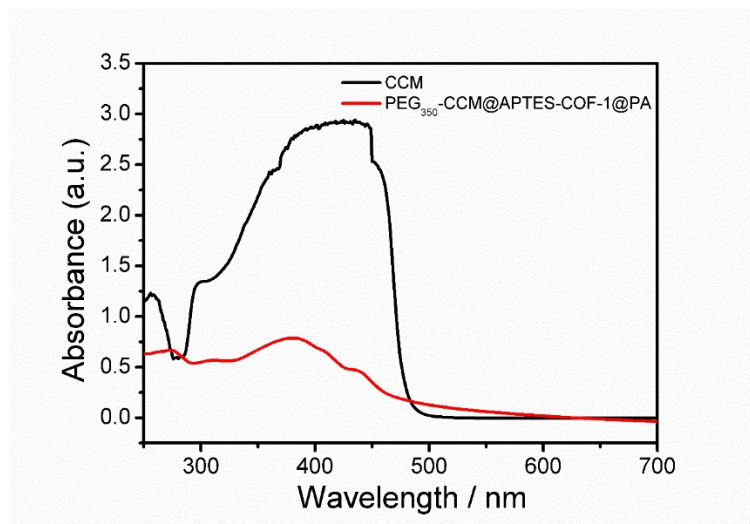


Figure S1. UV-vis spectra of the COF-based materials in methanol solution.

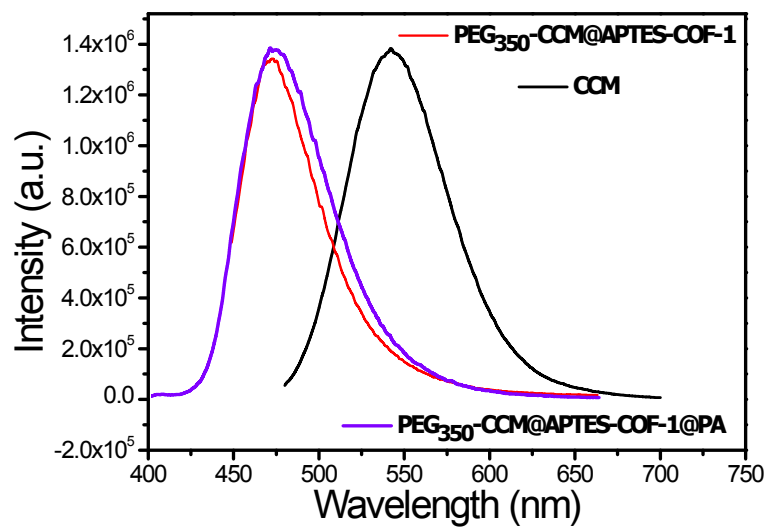


Figure S2. PL spectra of free CCM (black solid line) and PEG₃₅₀-CCM@APTES-COF-1@PA (red solid line).

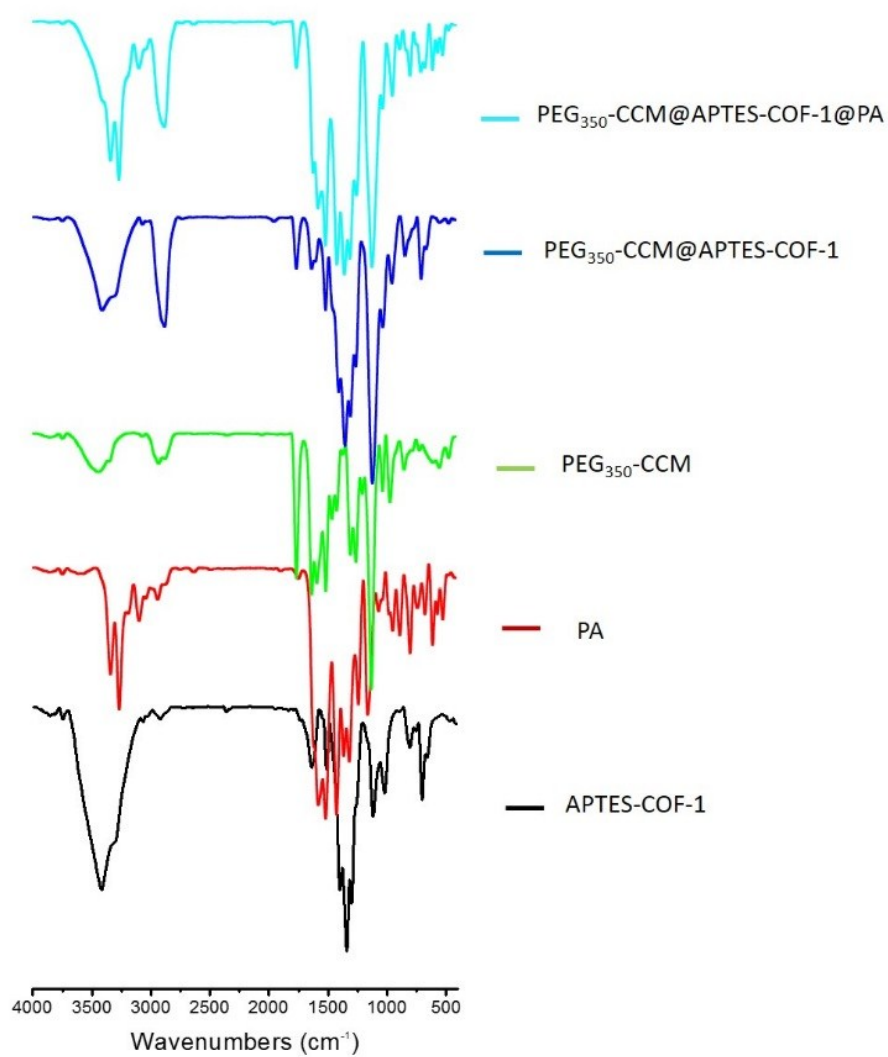


Figure S3. FT-IR spectra of APTES-COF-1, PA, PEG₃₅₀-CCM, PEG₃₅₀-CCM@APTES-COF-1, and PEG₃₅₀-CCM@APTES-COF-1@PA.

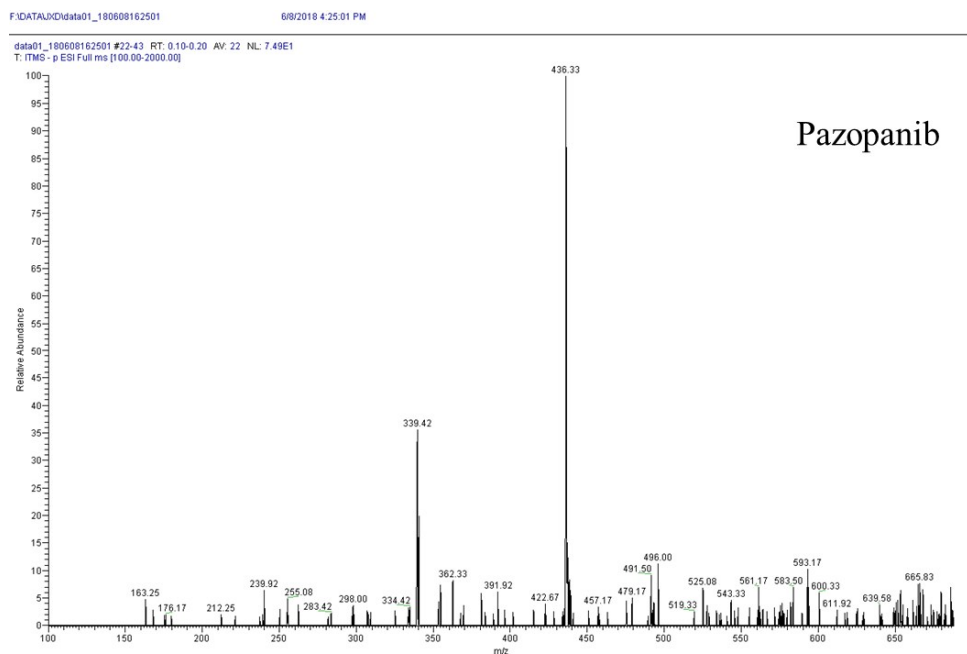


Figure S4. ESI-MS spectra of PA monomer.

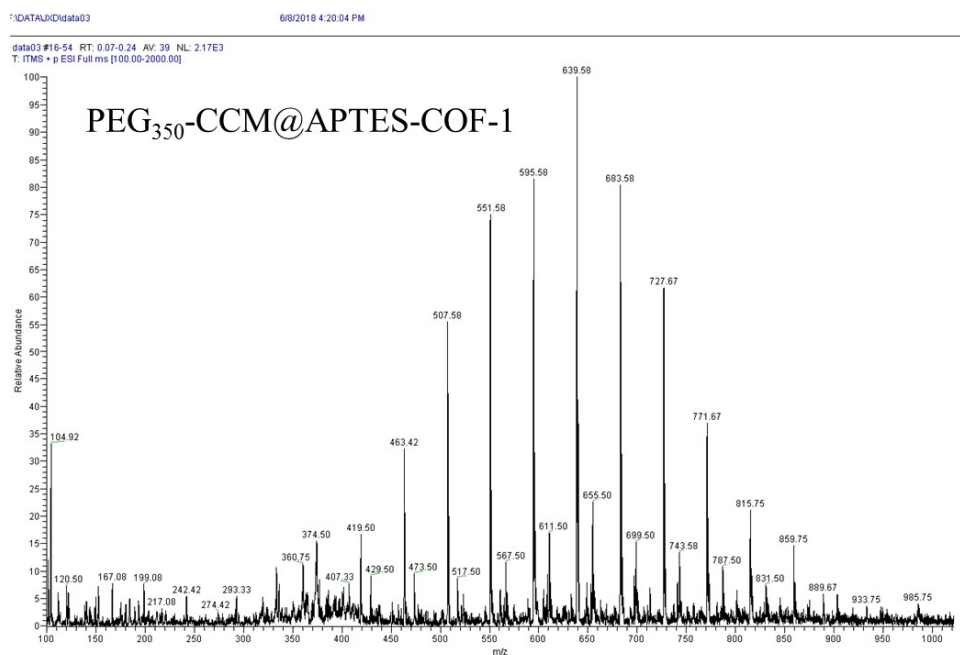


Figure S5. ESI-MS spectra of PEG₃₅₀-CCM@APTES-COF-1 monomer.

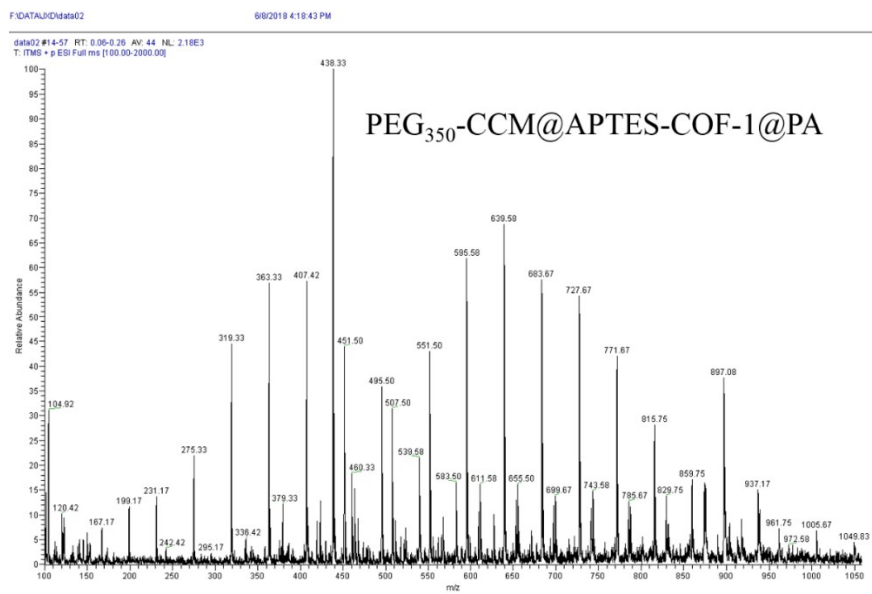


Figure S6. ESI-MS spectra of PEG₃₅₀-CCM@APTES-COF-1@PA monomer.

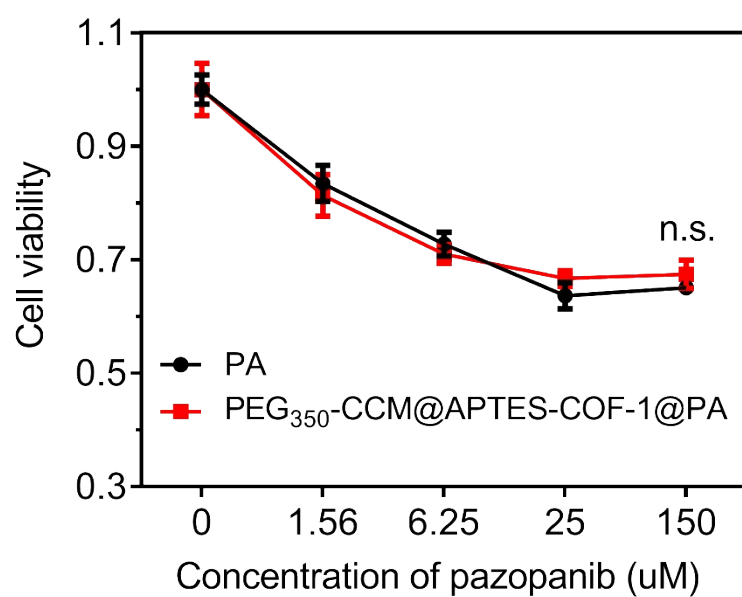


Figure S7. Cytotoxicity of PEG₃₅₀-CCM@APTES-COF-1@PA against renal cells (Renca) after 48 h- incubation at different concentrations. Error bars indicate s.d. (n=4). n.s. $P > 0.05$.

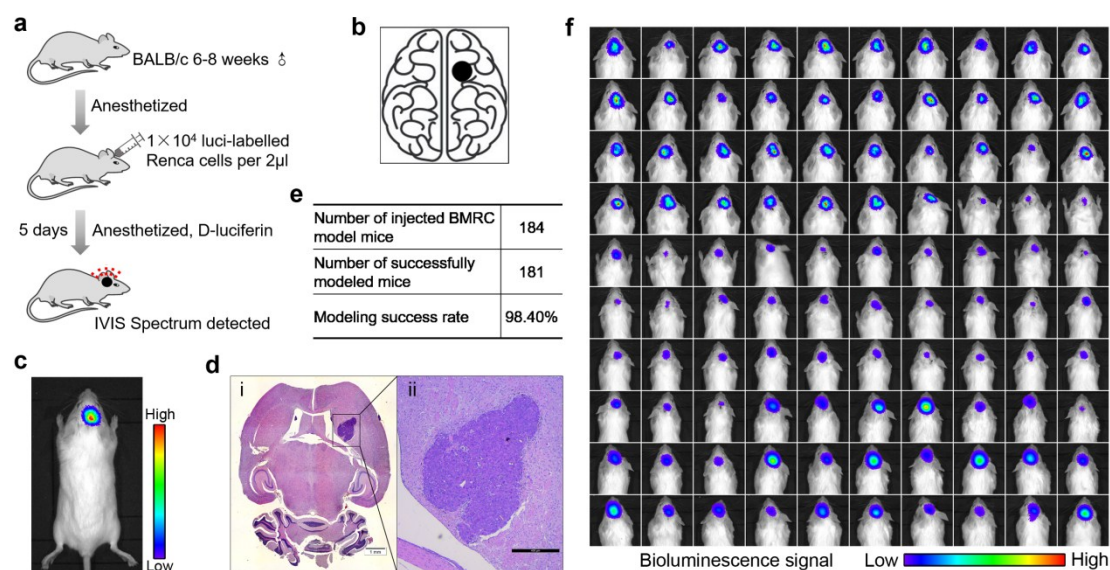


Figure S8. Establishment and verification of the intracranial BMRC model. **a** Schematic illustration of the construction of the intracranial BMRC model; **b** schematic diagram of the puncture point in the mouse brain; **c** representative bioluminescence image of one successfully established BMRC model five days after intracranial injection; **d** histopathological (H&E-stained) section of renal cancer cell growth in brain on the cross section (scale bars: (i) $1000 \mu\text{m}$ and (ii) $400 \mu\text{m}$); **e** statistical results of the BMRC model established in this study; **f** One hundred different representative *in vivo* bioluminescence images of successfully established BMRC mice (Statistics of 100 mice).

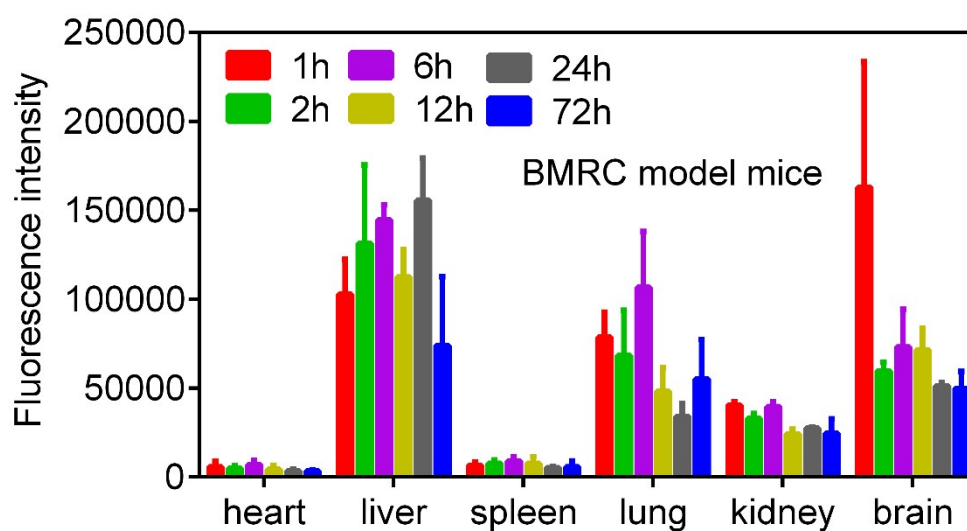


Figure S9. Region-of-interest analyses of absolute fluorescent signals from the BMRC mice. Tail injection into the mice was at a single sample dose of 50 mg kg^{-1} in PBS. Error bars indicate s.d. (n=2-3 independent experiments).

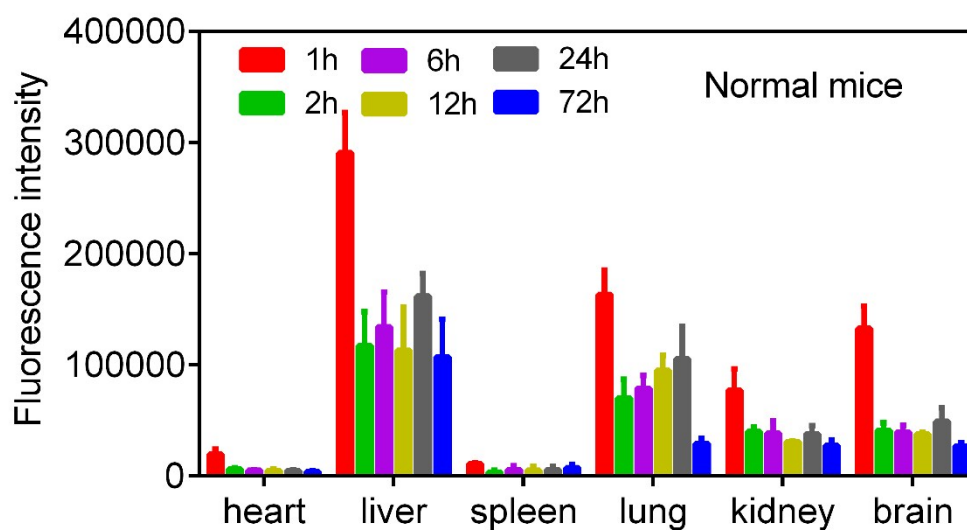


Figure S10. Region-of-interest analyses of absolute fluorescent signals from the normal mice. Tail injection into the mice was at a single sample dose of 50 mg kg^{-1} in PBS. Error bars indicate s.d. (n=2-3 independent experiments).

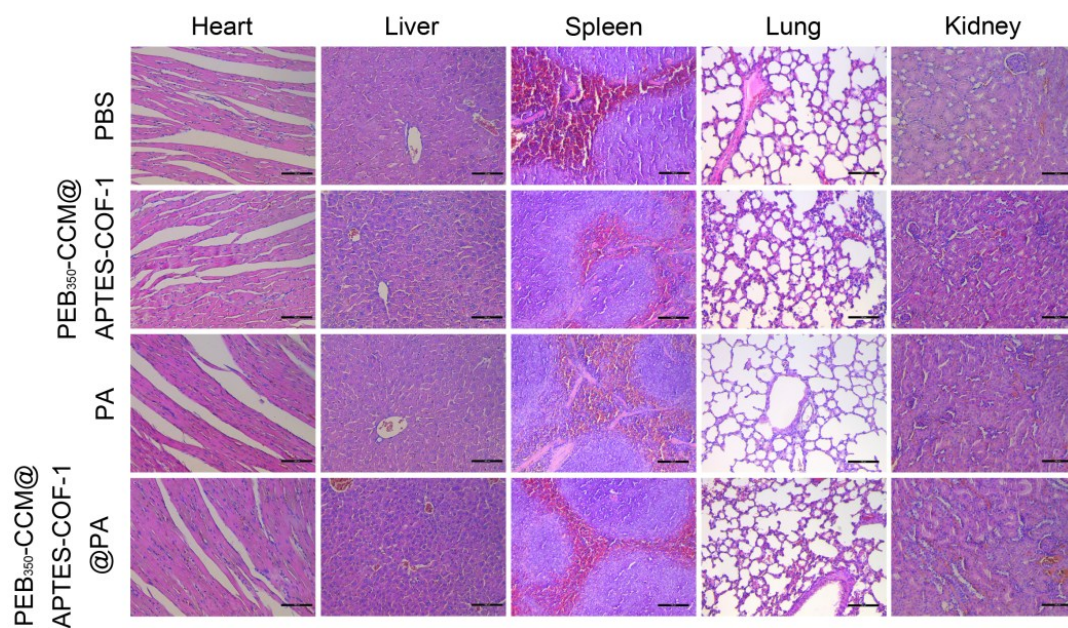


Figure S11. Biosafety analysis of PA-loaded naocomposites in tumor-bearing mice.

Pathological analysis of the H&E-stained main organs sections of mice treated with PBS, PEG₃₅₀-CCM@APTES-COF-1, PA, and PEG₃₅₀-CCM@APTES-COF-1@PA. No significant pathological change was observed in all of the organs. For all images: scale bar represents 100 µm.

Figure S12. Assay of PEG₃₅₀-CCM@APTES-COF-1@PA

Sample Name		Internal standard peak area (Ai)	API peak area (As)	As/Ai	Average	Sample weight (g)	Injection concentration ($\mu\text{g ml}^{-1}$)	PA content calculation	Average
Samples	PEG ₃₅₀ -CCM@APTES-COF-1@PA-1-1	496014	3993540	8.05	-	0.0100	-	46.05%	45.83%
	PEG ₃₅₀ -CCM@APTES-COF-1@PA-1-2	495851	3984327	8.04		0.0100	-	45.96%	
	PEG ₃₅₀ -CCM@APTES-COF-1@PA-2-1	497942	3979699	7.99		0.0100	-	45.72%	
	PEG ₃₅₀ -CCM@APTES-COF-1@PA-2-2	498436	3974442	7.97		0.0100	-	45.61%	
Control	PA-1-1	502213	4407382	8.78	8.74	0.0100	50	-	-
	PA-1-2	502289	4401708	8.76		0.0100	50	-	-
	PA-2-1	504576	4398433	8.72		0.0100	50	-	-
	PA-2-2	505471	4402298	8.71		0.0100	50	-	-